Micro-electrical Discharge Machining of Hard Brittle Materials

25

Pay Jun Liew and Jiwang Yan

Contents

Abstract

In recent years, the use of single crystals and ceramic materials such as silicon carbide (SiC), alumina, and silicon nitride has received intensive attention in mechanical and manufacturing engineering. However, due to their high

P. J. Liew (✉)
Manufacturing Process Department, Faculty of Manufacturing Engineering, Universiti Teknikal Malaysia Melaka, Hang Tuah Jaya, Melaka, Malaysia
e-mail: payjun@utem.edu.my

J. Yan
Department of Mechanical Engineering, Keio University, Yokohama, Japan
e-mail: yan@mech.keio.ac.jp

J. Yan (ed.), *Micro and Nano Fabrication Technology*, Micro/Nano Technologies,
https://doi.org/10.1007/978-981-13-0098-1_25

hardness, these materials are typically difficult to machine by mechanical machining methods. In particular, the fabrication of microstructures and high aspect ratio micro hole on these hard and brittle materials by using cutting and abrasive machining is very difficult and involves high production cost. As an alternative approach, micro-electrical discharge machining (micro-EDM) is effective. In this chapter, three major approaches that have been used by previous researchers to improve the EDM machinability of low conductivity and insulating ceramic materials such as powder mixed EDM, assisting electrode EDM and electrical discharge milling and grinding, will be overviewed. Then some newly developed technologies for machining hard and brittle materials by using micro-EDM will be introduced. One is hybrid micro-EDM by combining ultrasonic cavitation and carbon nanofibers. The effect of carbon nanofiber concentration and ultrasonic vibration on micro hole geometry, surface topography, and surface roughness will be described. By using the hybrid EDM process, high aspect ratio micro holes and micro dimples were successfully fabricated on RB-SiC. Another example is a hybrid tooling technology using polycrystalline diamond (PCD) for micro-EDM and grinding of single-crystal SiC. This enabled achieving extremely smooth surfaces in nanometer level after EDM.

Keywords
Micro-electrical discharge machining · Hard and brittle materials · Carbon nanofibers · Hybrid tool · Micro-structures

25.1 Overview of Electrical Discharge Machining

Electrical discharge machining (EDM), also known as spark machining, is an electrothermal machining process, whereby a desired shape is obtained using electrical discharges (sparks). In EDM, both electrode and workpiece are submerged in a dielectric fluid, which is generally kerosene or deionized water. During the process, there is no mechanical contact between the electrode and the workpiece. The electrical sparks are generated in a dielectric fluid by electrical energy and act as a cutting tool, to remove the workpiece material by melting and evaporation. The volume removed by a single spark is small, in the range of 10^{-6}–10^{-4} mm^3; however the sparks occur at a high frequency, typically 10,000 times per second (Descoeudres 2006).

The dielectric fluid plays an important role in the EDM process. According to Kalpakjian and Schmid (2001), the dielectric fluid acts as an insulator and flushing medium to carry away the debris and provide the cooling medium to the tool and the workpiece. The machining performance of EDM depends on many factors, such as electrode material, workpiece material, non-electrical machining parameters, and electrical machining parameters. Figure 1 shows the Ishikawa cause-effect diagram for EDM process.

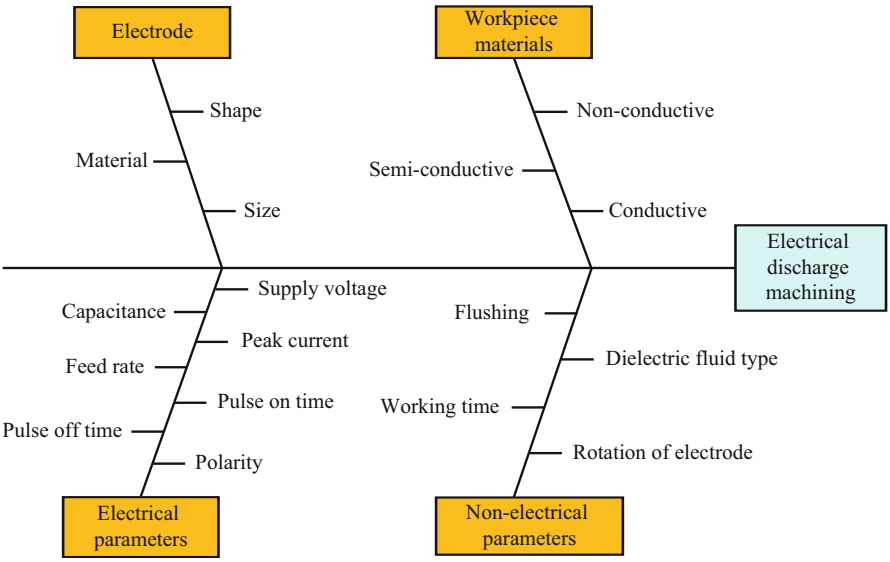

Fig. 1 Ishikawa cause-effect diagram of EDM process

25.1.1 Principle of EDM

According to Schumacher (2004), the sparking phenomena or electrical discharge during EDM can be separated into three important phases, namely, preparation phase for ignition, phase of discharge, and interval phase between discharges. Figure 2 gives an overview of the erosion process due to a single EDM discharge. The phenomena of sparking are briefly explained, as below:

(a) Voltage is applied between the electrode and the workpiece. At low electric current, electrons pass through the dielectric fluid from the negative electrode toward the positive workpiece and vice versa. An electric field or energy column is created.
(b) At the closest point between the electrode and workpiece, the breakdown of the dielectric fluid is initiated. When the breakdown occurs, the voltage falls and a current rises abruptly. A plasma channel (ionized, electrically conductive gas with high temperature) is created between the electrode and the workpiece.
(c) During the discharging phase, the discharge current is maintained to assure a continuous bombardment of ions and electrons on the electrodes. This will cause strong heating of the workpiece material and electrode material. As a result, small molten metal pool at the surface is created. A small quantity of metal can be directly vaporized due to the heating. The plasma channel expands and the vapor bubble grows. Therefore, the radius of the molten metal pool increases with time.
(d) At the end of the discharge, the current and the voltage are shut down. When the plasma is put off, the heat generation stops, and the pressure falls rapidly, but the

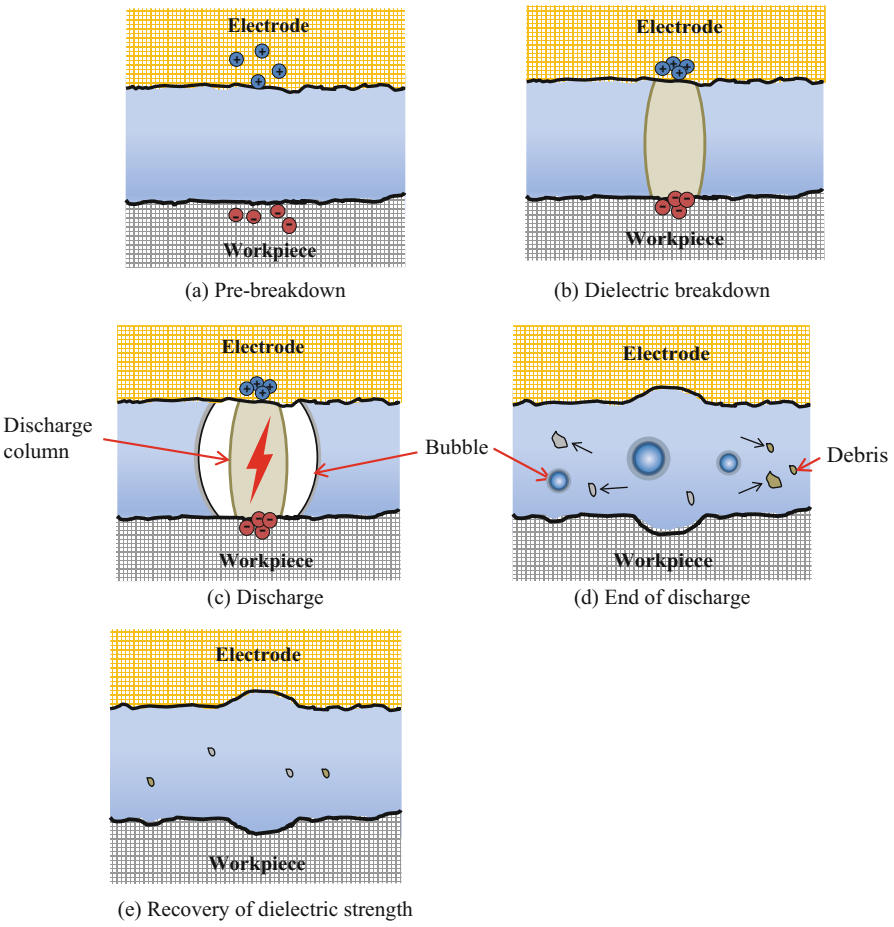

Fig. 2 Erosion process due to a single EDM discharge (Schumacher 2004, with permission from Elsevier)

vapor bubble continues to grow until it collapses to smaller bubbles. The plasma implodes under the pressure imposed by the surrounding dielectric. Consequently, the molten metals are evaporated and ejected into the dielectric, leaving a small crater at the workpiece surface (typically 1–500 μm in diameter, depending on the current).

(e) After the end of discharge, ions and electrons are recombined, and the dielectric breakdown strength is recovered.

25.1.2 Micro-EDM and Its Types

In principle, the mechanism of the micro-EDM process and macro-EDM process is similar. The main differences between these two processes are in the size of the tool

used, the power supply of discharge energy, and the resolution of the X-, Y-, and Z-axis movements (Masuzawa 2000). Zahiruddin and Kunieda (2012) reported that the significant difference between micro-EDM and macro-EDM was the power density. It was found that the power density of micro-EDM was approximately 30 times greater than that of macro-EDM. Consequently, energy efficiency and removal efficiency in micro-EDM were significantly greater than those of macro-EDM.

There are four different types of micro-EDM technologies which are used for manufacturing micro-features, namely, die-sinking micro-EDM (an electrode with micro-features is employed to produce its mirror image in the workpiece), micro-wire EDM (a wire is used to cut through a conductive workpiece), micro-EDM drilling (micro-electrodes are used to "drill" micro holes in the workpiece), and micro-EDM milling (micro-electrodes are employed to produce three-dimensional cavities by adopting a movement strategy similar to that in conventional milling) (Pham et al. 2004).

In the micro-EDM machine that was used in this chapter, two main types of machining can be distinguished, namely, die-sinking micro-EDM and wire electro-discharge grinding (WEDG). In die-sinking EDM, the workpiece is formed either by replication of the shaped tool electrode or by three-dimensional movement of a simple electrode. Normally, negative electrode polarity is used when performing a test using die-sinking EDM. Tungsten rod, which is shaped by WEDG, is normally used as an electrode and fed in the z direction, toward the workpiece that immersed in the dielectric fluid. Die-sinking EDM is mainly used to produce injection molds. WEDG, which was developed by Masuzawa et al. (1985), uses a brass wire to erode away material from a rotating workpiece to produce a cylindrical shaft. The workpiece (anode) is held vertically in a mandrel that rotates at 3000 rpm, and its position is slowly fed in the z direction. A φ100 μm brass wire (cathode) is supported on a wire guide, and its position is controlled in the x- and y-directions. The electrical discharges, which are produced by resistor-capacitor (RC), erode the material from the workpiece and the brass wire, within a small gap (~ 2 μm) filled with dielectric oil (Morgan 2004). WEDG has been widely adopted to fabricate micro-tool electrode for micro-EDM as well as other processes. Compared to serial machining with single tool electrode, machining by micro-tool electrode array has become an important topic in micromachining to improve throughput and precision (Chung et al. 2011). For example, Yi et al. (2008) successfully machined square hole by micro-EDM using 4 × 4 copper electrode array that fabricated by reserve EDM, as shown in Fig. 3. The results show that the productivity was improved to five times of that in the case using a single electrode.

25.1.3 Micro-EDM of Hard and Brittle Materials

Recently, micro-EDM has become popular to machine hard ceramic material. The growing popularity of micro-EDM can be attributed to its advantages, such as low installation cost and its ability to machine complex three-dimensional shapes easily regardless of material hardness (Reynaerts et al. 1998). Furthermore, during machining with micro-EDM, there is no direct contact between the electrode and

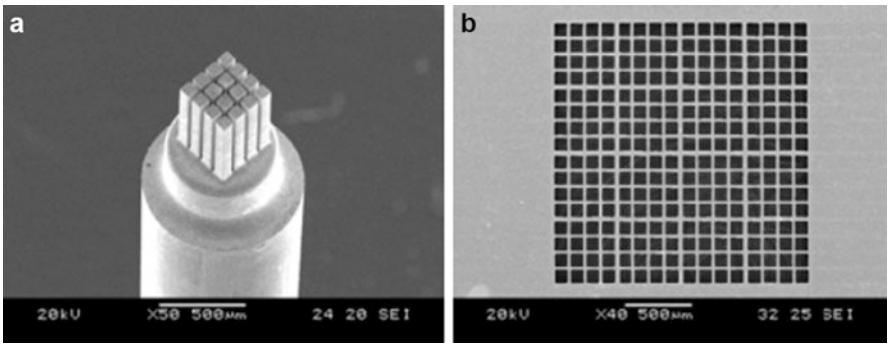

Fig. 3 (**a**) A 4 × 4 Cu electrode array fabricated by reverse EDM, (**b**) square holes by micro-EDM using the 4 × 4 Cu electrode array (Yi et al. 2008, with permission from Springer)

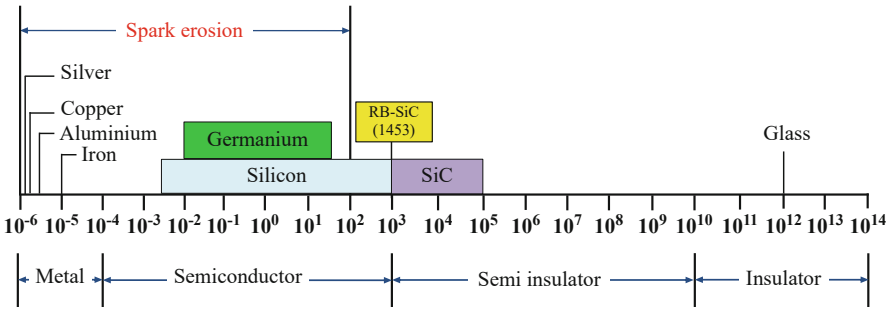

Fig. 4 Resistivity of various materials (Ωcm) (Lee et al. 2013, with permission from Elsevier)

workpiece, thus eliminating mechanical stress, chatter, and vibration problems (Ho and Newman 2003). EDM has been used extensively for machining various ceramic materials. For example, a comparative study of the die-sinking EDM of three different ceramic materials was carried out by Puertas and Luis (2004). Clijsters et al. (2010) also manufactured complex parts on SiSiC materials using EDM. When machining hard and brittle ceramic materials by EDM, information about the workpiece conductivity/resistivity is therefore an absolute prior requirement. The resistivity of the workpiece is a limiting factor for the discharge current, which directly affects the material removal rate (Lee et al. 2013). Various materials with their resistivity are shown in Fig. 4. As mentioned earlier, 100 Ωcm is the upper limit of electrical resistivity for a ceramic workpiece to be machined by EDM (Konig et al. 1988). However, most ceramics are not sufficiently conductive, which is a major problem when applying EDM to ceramic materials. For example, the reaction bonded silicon carbide (RB-SiC) ceramic material that was used in this chapter possesses a very high electrical resistivity, which is around 1453 Ωcm.

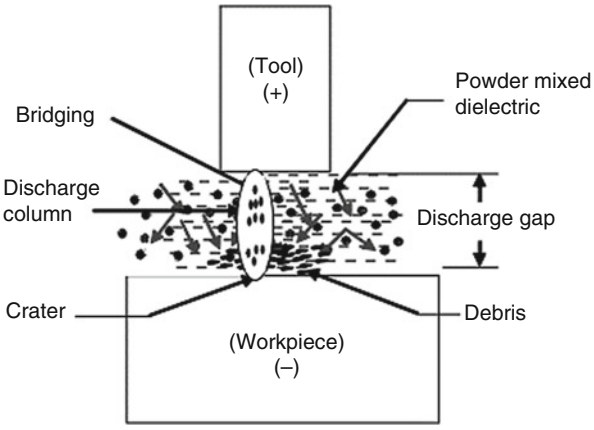

Fig. 5 Principle of powder mixed EDM (Kansal et al. 2007, with permission from Elsevier)

It is typically difficult to be machined directly by EDM. Hence, the method for increasing the EDM machinability of materials is crucial. From the past researches, several methods have been used, as summarized in the following subsections.

25.1.3.1 Powders Mixed EDM

The mechanism of powder mixed EDM (PMEDM) is different from the conventional EDM with the pure dielectric fluid. In powder mixed EDM, suitable conductive materials in the form of powders are mixed into the dielectric fluid, as schematically shown in Fig. 5. Under the influence of high potential intensity, the particles are charged and accelerated, move in the zigzag fashion, and may act as conductors. At the sparking gap between electrode and workpiece, the particles arrange themselves in the form of chain-like structures and interlock to each other in the direction of flow of current. The chain formation helps in bridging the discharge gap, and subsequently, the insulating strength of the dielectric fluid decreases due to the bridging effect. Thus, discharge column is easily formed, and short circuit is easy to take place, leading to early explosion in the gap (Kansal et al. 2007). A smaller crater size is created due to the gap enlargement and high frequency of discharge. The flowing powder additive creates another bridging effect, discharge column, and lastly explosion. The discharging processes repeat continuously until the final shape is obtained.

Powder mixed EDM proved to be an effective process to improve the machining efficiency and surface finish of materials. For example, Yeo et al. (2007) added 45–55-nm-sized SiC powders into dielectric, and they found that the surface craters became smaller than those produced in powder-free dielectric fluid. Chow et al. (2008) added SiC powders into pure water as dielectric fluid in the EDM of titanium alloy and confirmed the improvement in surface quality and material removal rate. Gunawan et al. (2009) added molybdenum disulfide (MoS_2)

powders and improved the material removal rate and surface roughness of Cu, brass, and Cu-W workpiece materials. Gunawan et al. (2011) also tried suspending nano graphite powders in dielectric fluid with the combination of ultrasonic vibration. They found that the machining time was reduced up to 35%.

Powder mixed EDM was also applied to the EDM of ceramic materials. Jahan et al. (2010a, b) studied the effect of adding graphite, aluminum, and nonconductive alumina powders in EDM of tungsten carbide ceramics. They found that the graphite powders provided a smooth surface and the aluminum powders resulted in higher spark gap and higher material removal rate, whereas the alumina powders had little effect on the EDM performance. Nevertheless, for low conductivity or insulating ceramic materials, it was difficult to obtain good machining performance by powder addition. For example, Tani et al. (2002) used Al, Gr, Si, Ni, and ZrB_2 powders to assist the EDM of insulating Si_3N_4 ceramics and found that even though the removal rate was increased, the surface roughness was barely improved. This was due to the generation of long pulse discharge in the EDM process.

25.1.3.2 Assisting Electrode EDM

Pioneer work can be traced to Mohri et al. (1996), who developed a new method of machining insulating ceramic material by EDM. It is called assisting electrode method. In this method, a metal plate or metal mesh is arranged on the surface of ceramic insulator as an assisting electrode. The machining process is shown in Fig. 6. In the early stage, discharges are generated between the metal plate and tool electrode. When the metal plate is eroded, the dielectric oil is thermally decomposed. Cracked carbon from the working oil and other electrical conductive compounds from the metal plate are deposited on the surface of ceramics. It keeps electrical conductivity on the surface of the workpiece during the machining. Hence, discharge continues to occur over the ceramics.

Figure 7 shows the machining apparatus for the assisting electrode method by WEDM. By using this method, insulating ceramics such as alumina and Si_3N_4 have been machined by sinking EDM (Muttamara et al. 2003; Fukuzawa et al. 2004; Muttamara et al. 2009). In addition, Tani et al. (2004) and Fukuzawa et al. (2009) fabricated three-dimensional complex shape successfully on the insulating Si_3N_4 and ZrO_2 with this assisting electrode method by WEDM. Sabur et al. (2013) also machined nonconductive ceramic ZrO_2 using assisting electrode by EDM. The experimental results show that the material is removed in EDM of nonconductive ZrO_2 ceramic mostly by spalling, and it increases with the increase of input power. Recently, Gotoh et al. (2016) also used the long pulse discharge in WED-milling to machine insulating ceramic Si_3N_4. With this long pulse discharge, an electrical conductive layer is formed on the surface of the insulating ceramic, which maintains stable machining.

25.1.3.3 Electrical Discharge Milling and Mechanical Grinding

In order to improve the EDM machinability of high resistivity of ceramic material, a new compound machining process that integrates electrical discharge (ED) milling and mechanical grinding is proposed (Liu et al. 2008). The principle for ED milling

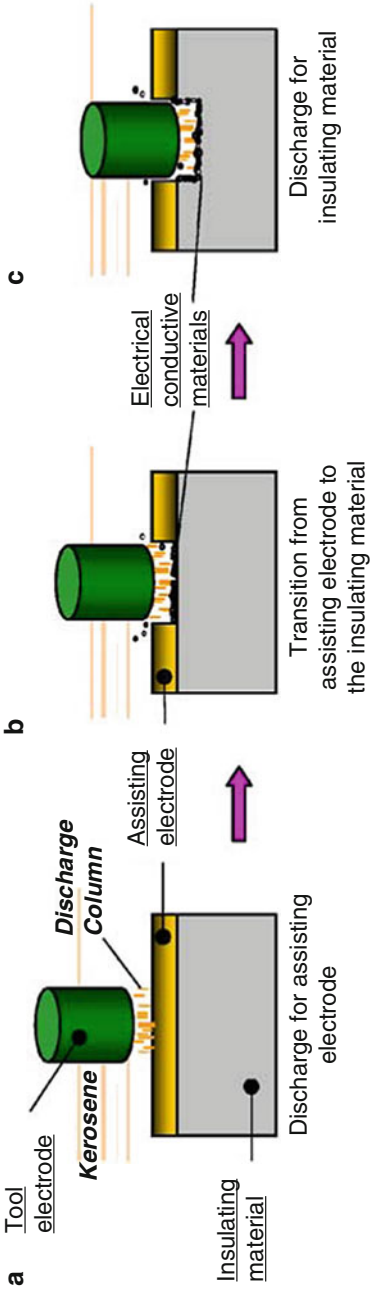

Fig. 6 Machining process of insulating materials using assisting electrode (Fukuzawa et al. 2004, with permission from Elsevier)

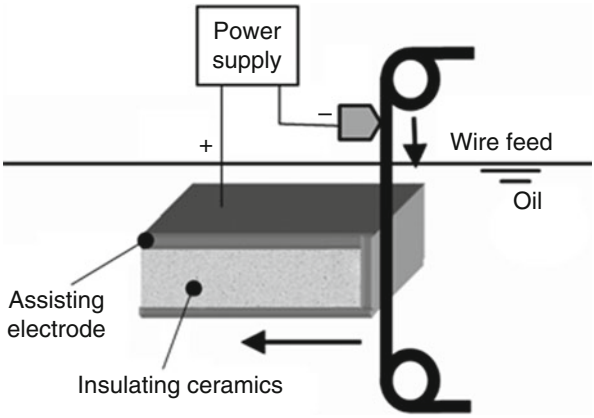

Fig. 7 WEDM of insulating ceramics (Fukuzawa et al. 2009, with permission from Elsevier)

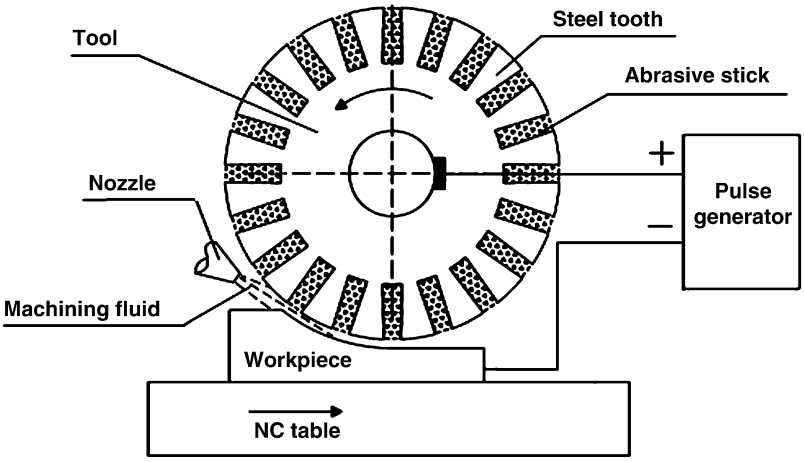

Fig. 8 ED milling and mechanical grinding (Ji et al. 2010, with permission from Sage Publications)

and mechanical grinding is shown in Fig. 8. In this hybrid process, the tool and the workpiece are connected to the positive and the negative poles of the pulse generator, respectively. Steel wheel with teeth is used as a tool. During machining, the tool rotates at a high speed on a rotary spindle which is driven by an AC motor. The water-based emulsion machining fluid is flushed into the gap with a nozzle, and the ceramic workpiece is fed toward the tool with an NC table. Electrical discharges are produced when the distance between the workpiece and the steel tooth reaches the discharge gap and caused the ceramic to be removed by ED milling. With a steel toothed wheel as the tool electrode, high resistivity SiC ceramic can be easily machined by ED milling (Liu et al. 2009; Ji et al. 2010, 2011).

The aforementioned methods are the three major approaches that have been used by the previous researchers to improve the EDM machinability of low conductivity and insulating ceramic materials. In this chapter, new machining method will be developed for increasing the machining efficiency of RB-SiC by using micro-EDM while maintaining the surface integrity and dimensional accuracy of machined microstructures.

25.2 Carbon Additive Assisted Micro-EDM of RB-SiC

For improving the machining efficiency of RB-SiC, carbon additive assisted micro-EDM of RB-SiC was proposed (Liew et al. 2013a). In this experiment, two different types of additives, namely, spherical carbon powders and cylindrical carbon nanofibers, were added into the dielectric fluid, respectively. The spherical carbon was in 150 nm cluster size, while the carbon nanofiber was 150 nm in diameter and 6–8 μm in length. The effect of these additives on the spark gap and material removal rates was investigated experimentally.

25.2.1 Machining Equipment and Conditions

Micro-EDM test was performed on the sample using a micro-EDM machine Panasonic MG-ED82W. Tungsten rods with 300 μm diameters were used as tool electrodes. Each test was run on the sample for a duration of 5 min, and average of three tests for each parameter setting was taken. The dielectric fluid used was hydrocarbon dielectric oil CASTY-LUBE EDS, which has a high flash point. Before the experiment, the required amounts of additives and dielectric fluid were measured separately before being mixed together and homogenized in a mixer for 20 min. This is to ensure that the carbon nanofibers are dispersed uniformly in the dielectric fluid. Table 1 summarizes the experimental conditions.

25.2.2 Result and Discussion

25.2.2.1 Spark Gap

Figure 9 shows the effect of carbon additives on spark gap. It indicates that the spark gap increases with the increase of spherical carbon powders and carbon nanofiber concentrations. Moreover, it is worth noting that carbon nanofiber could produce bigger spark gap compared to the one obtained with addition of spherical carbon powders. Presumably, when carbon nanofibers were added into the dielectric fluid, long and thin carbon nanofibers might be able to bridge the gap between the electrode and workpiece more significantly by interlocking to each other if compared to round-shaped carbon powders. Furthermore, the high electrical conductivity of

Table 1 Experimental conditions

Rotational speed	3000 rpm
Voltage	110 V
Condenser capacitance	3300 pF
Feed rate	3 μm/s
Dielectric fluid	EDM oil CASTY-LUBE EDS
Additive	Carbon nanofibers (CNFs) Carbon powder
Concentrations	0, 0.06, 0.14 g/L
Machining time	5 min

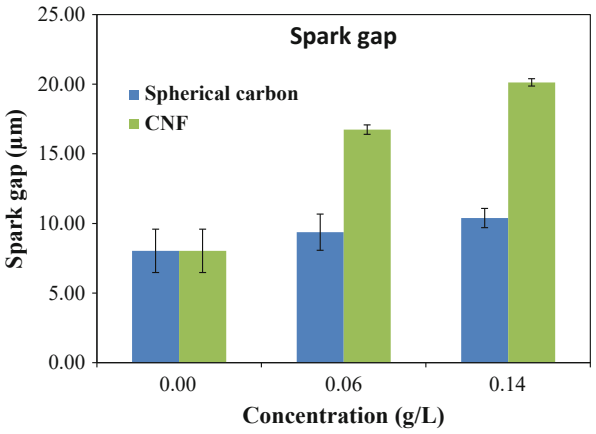

Fig. 9 Effect of spherical carbon powders and carbon nanofibers on spark gap

carbon nanofiber might help to reduce the insulating strength of the dielectric fluid, resulting in bigger sparking gap compared to the one obtained with spherical carbon powders.

25.2.2.2 Material Removal Rate

Figure 10 shows the effect of spherical carbon powders and carbon nanofibers on material removal rates (MRR). Clearly, with the addition of carbon nanofibers, the material removal rate is six to ten times higher than the one obtained with spherical carbon powders, especially at high concentration of additive. This result demonstrated that the frequency of discharge might be increased by the addition of carbon nanofibers. In addition, the sparking gap that is induced by the spherical carbon powders as mentioned in previous paragraph is typically lower than that of carbon nanofibers; thus, the debris may not be removed easily from the machining gap and cause an unstable machining which leads to the reduction of material removal rates.

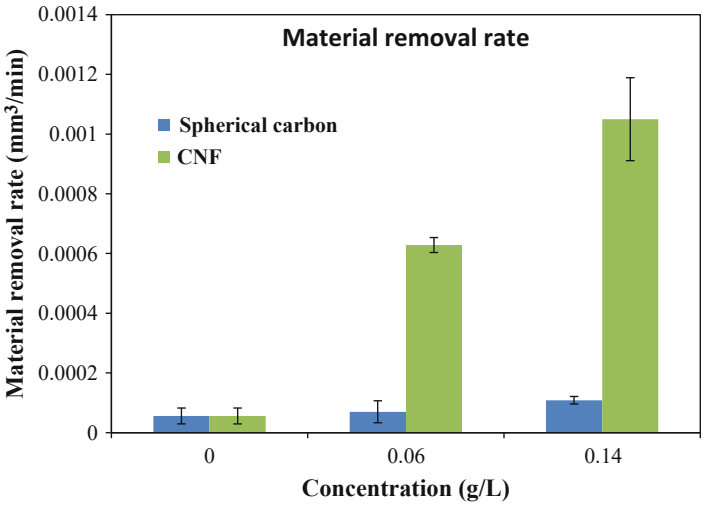

Fig. 10 Effect of spherical carbon powders and carbon nanofibers on material removal rate

Based on the aforementioned results, it is proved that carbon nanofiber additives are more effective in increasing the spark gap than the spherical powders. Subsequently, the debris can be removed easily, and material removal rates can be improved to a significant degree.

25.3 Ultrasonic Cavitation Assisted Micro-EDM

In recent years, the industrial demand for microstructural surface such as microgroove, microlens array, micropyramid arrays, and microprism array has been steadily increasing. Due to the wide applications of these functional microstructured surfaces in optical and biomedical engineering and microelectromechanical systems (MEMS), precision manufacturing process becomes essential to produce these microstructured surfaces, not only in terms of dimension and shape but also in the roughness quality of the machined surface (Hung et al. 2006).

Micro-EDM has gained an interest from many researchers as a precision machining tool for producing micro-features, such as fabrication micromolds for plastic lenses and glass, micro holes, microgrooves, and micro dimples. The growing popularity of micro-EDM can be attributed to its advantages, such as low installation cost (Reynaerts et al. 1998) and it can machine complex three-dimensional shapes easily regardless of material hardness. Furthermore, during machining with micro-EDM, there is no direct contact between the electrode and workpiece, thus eliminating mechanical stress, chatter, and vibration problems (Ho and Newman 2003).

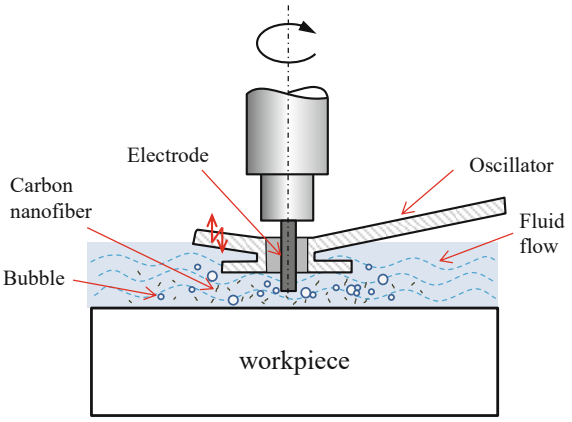

Fig. 11 Schematic diagram of cavitation assisted micro-EDM

However, due to the narrow sparking gap in micro-EDM, the removal of debris remains a challenging issue, especially in deep hole machining and fine finishing with lower discharge energy. In this chapter, a hybrid EDM process by combining ultrasonic cavitation and carbon nanofiber addition is proposed to improve machining efficiency, surface quality, and form accuracy of deep micro holes in RB-SiC ceramic material (Liew et al. 2014). Ultrasonic vibration was directly applied to the dielectric fluid in the machining region by using a probe-type vibrator (instead of vibrating the dielectric tank) to generate cavitation to assist micro-EDM of deep micro holes in RB-SiC. The effect of ultrasonic vibration was investigated in combination with the addition of carbon nanofibers into dielectric fluid.

Figure 11 shows the schematic diagram of cavitation assisted micro-EDM. In this method, a suitable amount of carbon nanofibers is added and mixed in the dielectric fluid, and then a probe-type oscillator horn is placed into the dielectric fluid over the workpiece. When ultrasonic vibration is applied to the dielectric fluid, intense ultrasonic waves travel through the liquid, generating small cavities that enlarge and collapse. This phenomenon is called as cavitation (Suslick 1989). Normally, in micro-EDM, the debris is removed by the gaseous bubbles escaping from the working area through the narrow discharge gap (Yu et al. 2009; Wang et al. 2012). In this chapter, instead of gaseous bubbles, the ultrasonic cavitation will dominate the removal of discharge-induced debris. Thus, stable machining performance might be obtained. Moreover, the ultrasonic vibration of dielectric fluid might prevent the carbon nanofibers from accumulating, so that the carbon nanofibers will disperse evenly in the dielectric fluid. As a result, frequency of electro discharge in the EDM of RB-SiC might be improved.

25.3.1 Machining Equipment and Condition

As the ultrasonic vibration device, SC-450 cavitation generator (Taga Electric Co., Ltd, Japan) with a power output of 50 W was used in this experiment. It has vibration

Table 2 Experimental conditions

Rotational speed	3000 rpm
Voltage	80 V, 100 V
Condenser capacitance	Stray capacitance (~ 1 pF), 3300 pF
Feed rate	3 μm/s
Vibration frequency	20 ± 1.5 kHz
Vibration amplitude	0~14 μm
Working distance	1~4 mm
Dielectric fluid	EDM oil CASTY-LUBE EDS
Additive CNFs size Concentration	Carbon nanofibers (CNFs) Diameter = 0.15 μm Length = 6~8 μm 0.06 g/L
Machining time	30~150 s

frequency of 20 kHz and maximum amplitude of 14 μm. The electrode was inserted through the hole at the end of the oscillator horn of a cavitation generator during the EDM process. The ultrasonic vibration was applied to the dielectric fluid by the oscillator horn, to cause the cavitation effect. The oscillator horn was placed approximately 2–3 mm from the workpiece.

With the roughing parameters, the changes in the micro hole geometry, surface topography, and surface roughness were investigated experimentally. For comparison, three types of micro-EDM tests were then carried out, namely, (1) carbon nanofibers addition in EDM oil only, (2) ultrasonic cavitation in pure EDM oil, and (3) combination of ultrasonic cavitation with addition of carbon nanofibers in EDM oil. Micro hole machining was performed on the sample for duration of specified time, and each parameter setting was repeated for three times. After each EDM cycle, electrode dressing was performed by using wire electro-discharge grinding (WEDG) in order to improve their form accuracy. Table 2 shows the experimental conditions.

25.3.2 Results and Discussion

25.3.2.1 Micro Hole Geometry

Micro hole geometry after EDM was investigated. Figure 12 presents SEM micrographs of machined micro hole obtained under various machining conditions. Figure 13a–c shows three typical cross-sectional profiles corresponding to the micro hole shown in Fig. 12a–c, respectively. The profiles were measured by laser probe profilometer NH-3SP. It is clear that with addition of carbon nanofibers but without ultrasonic cavitation (Fig. 12a), a cone-shape protrusion was formed in the center of the micro hole. In the sparking gap, the stagnation of debris occurs intensively around the center of the micro-cavity, where the debris particles interact with the tool electrode (Ekmekci and Sayar 2013), causing concavity at the center

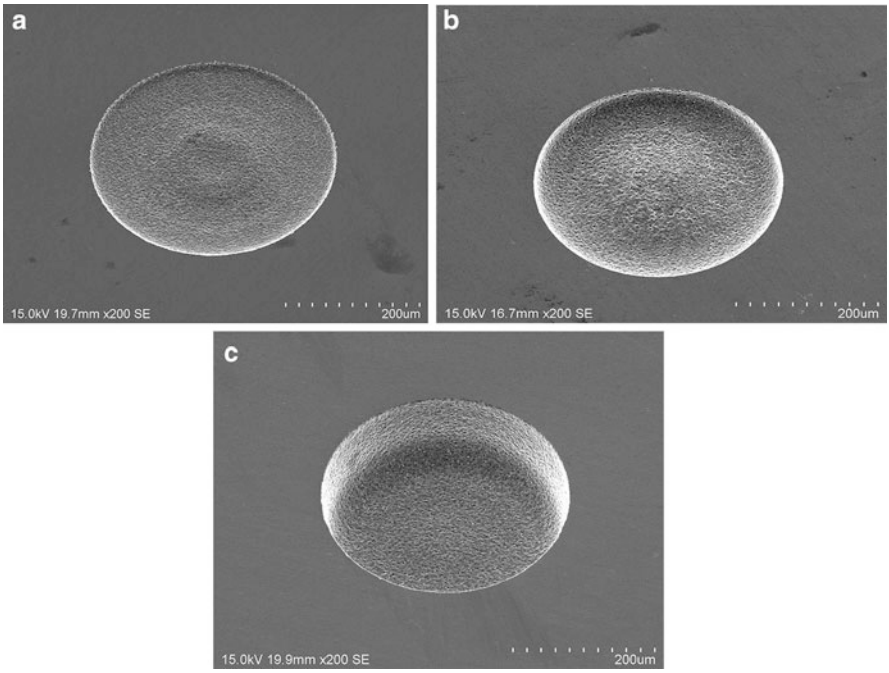

Fig. 12 SEM micrograph of micro hole after machining time of 2 min: (**a**) with 0.06 g/L carbon nanofibers only, (**b**) with ultrasonic cavitation in pure EDM oil, and (**c**) with ultrasonic cavitation and carbon nanofibers

of tool tip, and in turn, a cone-shape protrusion was formed at the bottom of the micro hole. The cone-shape protrusion was formed also when the ultrasonic cavitation was applied to the pure EDM oil (Fig. 12b). However, as shown in Fig. 12c, the cone-shape protrusion was insignificant, that is the bottom of micro hole became flat, when combination of ultrasonic cavitation and carbon nanofibers was used. At the same time, the depth of micro hole is deeper, as shown in Fig. 13. Carbon nanofibers addition in the dielectric fluid reduces the insulating strength of the dielectric fluid, causing a bigger discharge gap between the tool electrode and the workpiece. Thus, debris will be flushed out effectively with the help of cavitation bubble, and piled debris density in the center of micro hole will be prevented. This indicates that combination of ultrasonic cavitation and addition of carbon nanofibers in the dielectric fluid is more helpful for improving the form accuracy of the micro hole than EDM with the aid of either one exclusively.

25.3.2.2 Surface Topography

Figure 14 shows SEM micrographs of the machined surface obtained under various machining conditions. It is seen that with ultrasonic cavitation in pure EDM oil

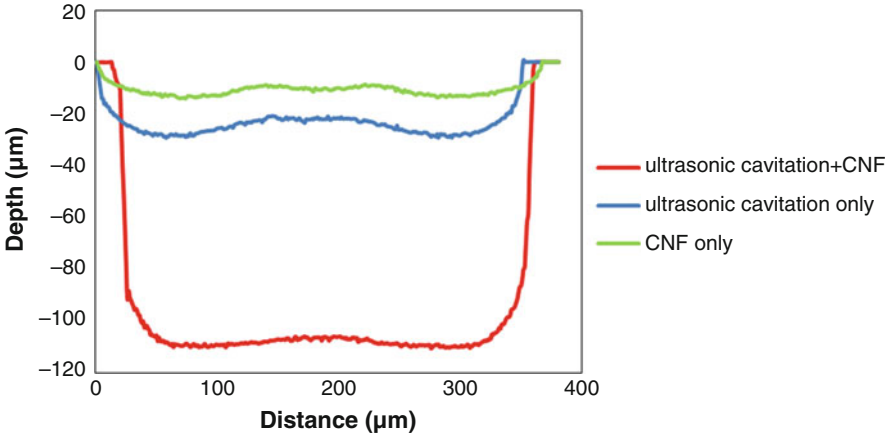

Fig. 13 Comparison of cross-sectional profiles of machined micro hole under various conditions

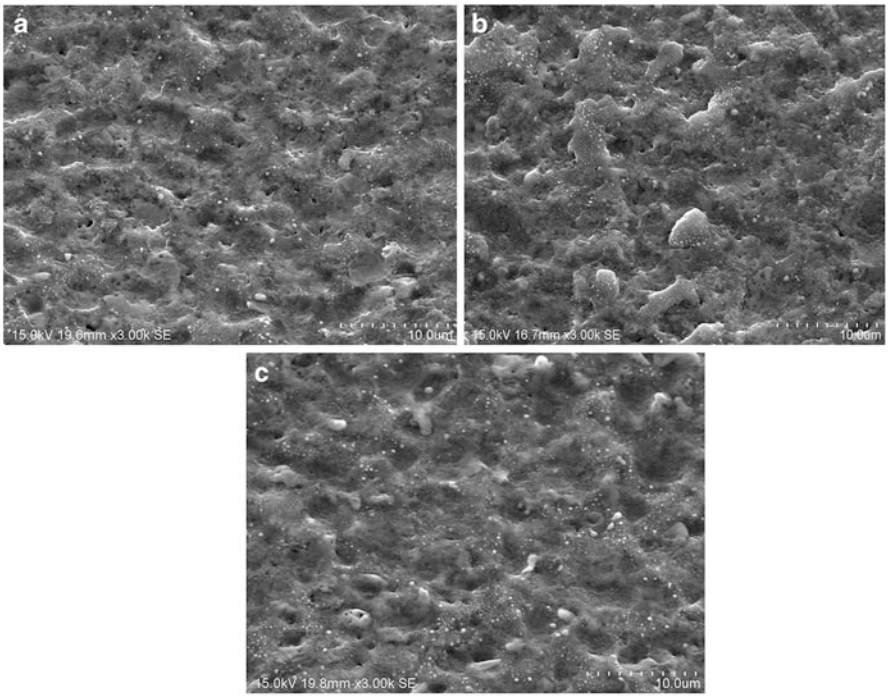

Fig. 14 Comparison of machined surface after machining time of 2 min: (**a**) with 0.06 g/L carbon nanofibers only, (**b**) with ultrasonic cavitation in pure EDM oil, and (**c**) with ultrasonic cavitation and carbon nanofibers

(without the carbon nanofiber addition), the surface of the micro hole was very rough and covered with resolidified material (Fig. 14b). In contrast, the machined surface in Fig. 14a and b were smoother, and surface craters became remarkably smaller. In this case, the material removal mechanism of RB-SiC involves spalling of large flakes, which is different from the other conductive materials. For this reason, we can say that the effect of ultrasonic cavitation only is insignificant for improving the surface topography of RB-SiC.

Next, laser probe profiling system was used to measure the surface roughness of the machined surface. Figure 15a–c shows three typical surface roughness profiles with the same scale corresponding to the micro hole shown in Fig. 12a–c, respectively. The minimum surface roughness is 0.2002 nmRa, which was obtained under the conditions of combination of ultrasonic cavitation and carbon nanofibers addition (Fig. 15c).

The vibration of dielectric fluid avoids the settling of carbon nanofibers at the bottom of the tank and induces multiple fine discharge, resulting better surface topography. At the same time, vibration-induced cavitation bubbles help to reduce the adhesion of resolidified debris on the machined surface. The surface roughness obtained with addition carbon nanofibers (Fig. 15a) was slightly higher (0.2173 nmRa). The roughest surface is 0.2814 nmRa obtained under the machining condition of ultrasonic cavitation in pure dielectric fluid. From these results, it can be easily elucidated that the hybrid process of ultrasonic cavitation and carbon nanofibers addition in the dielectric fluid is helpful for improving the surface finish of RB-SiC.

25.3.2.3 Process Mechanism

Figure 16 shows the schematic model for debris removal through the cavitation assisted micro-EDM with carbon nanofibers' addition in the dielectric fluid. Due to the pressure fluctuation in dielectric fluid which is induced by low-intensity ultrasonic waves, the generated cloud cavitation tends to oscillate at the working area. In a cloud cavitation, the nonlinear bubble dynamics produce nonlinear interactive effects which cause cascading of fluctuation energy (Kumar and Brennen 1991; Brennen 1995). Due to this fluctuating energy in the dielectric fluid, the debris might be flushed out from the gap easily. In some circumstances, as shown in Fig. 16, the cavitation bubbles might be initiated at the sparking gap between the electrode and workpiece during discharging phase, due to the pressure wave that propagates in the dielectric fluid. In this way, the debris will be ejected easily through the fluctuating cavitation bubbles, and instead, improving the machining efficiency of RB-SiC. In addition, the vibration of dielectric fluid uniformly disperses the carbon nanofibers and helps to activate the discharges, leading to a better surface finish and high material removal rate.

25.3.2.4 Fabrication of High Aspect Ratio Micro Hole

Next, hybrid EDM of ultrasonic cavitation and carbon nanofiber addition in dielectric fluid was applied to fabricate high aspect ratio micro holes on RB-SiC. Tungsten

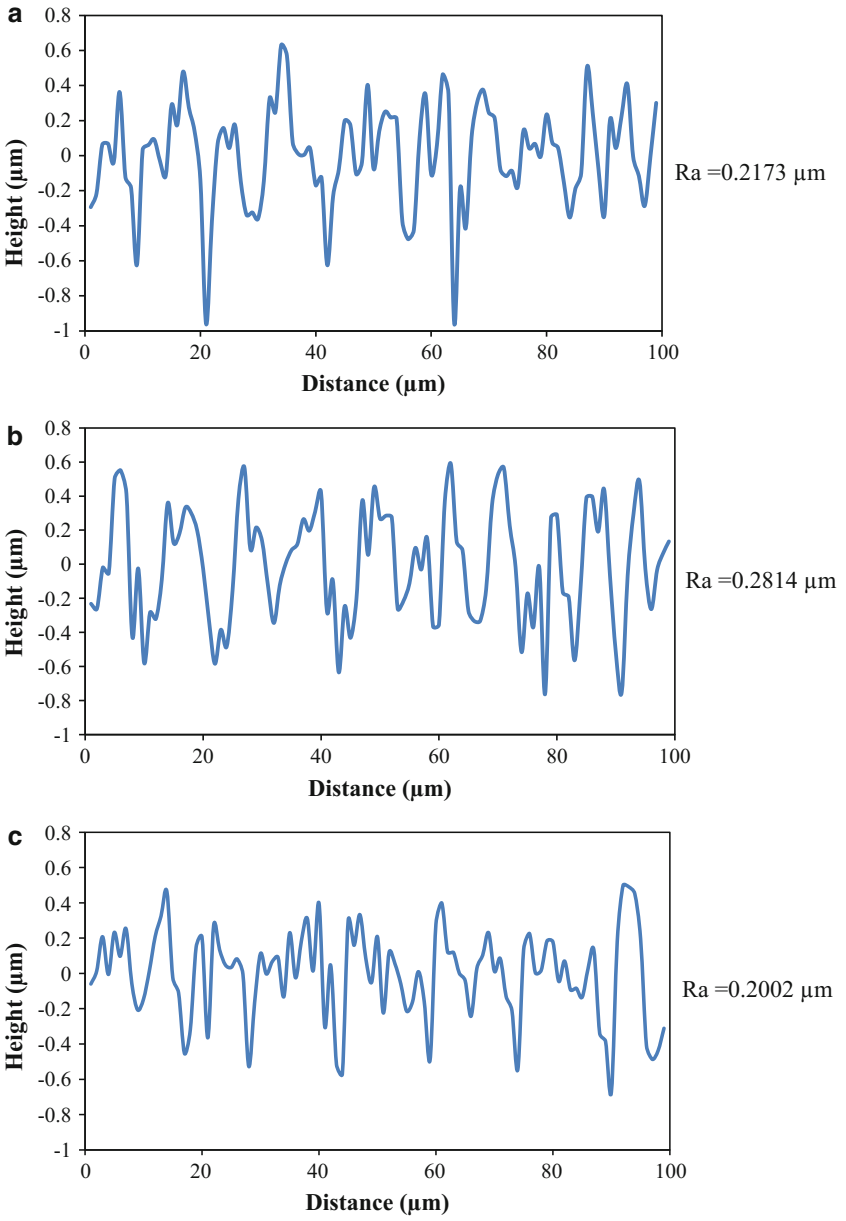

Fig. 15 Surface roughness profile: (**a**) with 0.06 g/L carbon nanofibers only, (**b**) with ultrasonic cavitation in pure EDM oil, and (**c**) with ultrasonic cavitation and carbon nanofibers

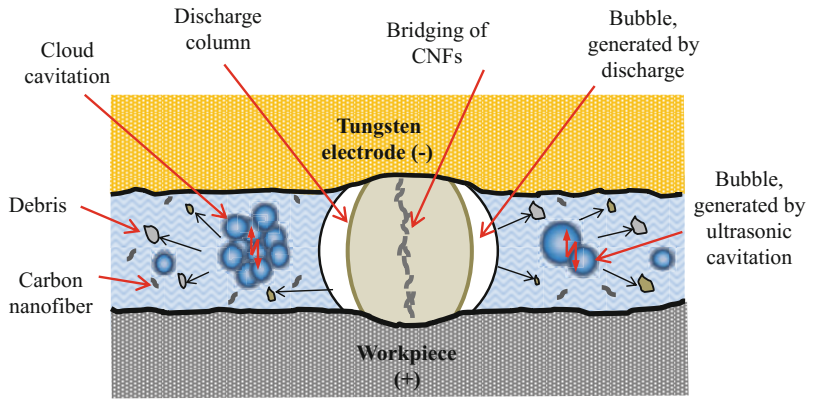

Fig. 16 Schematic model of debris removal with ultrasonic cavitation and addition of carbon nanofibers, through oscillation of cloud cavitation and cavitation bubbles that initiated during discharging phase

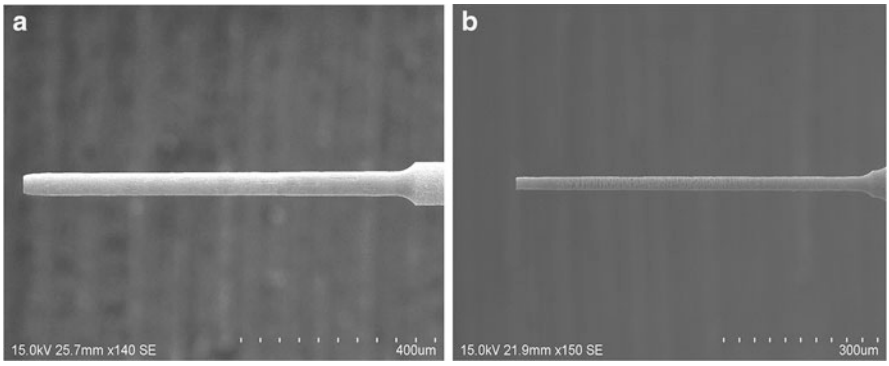

Fig. 17 Microelectrodes: (**a**) 50 μm diameter, (**b**) 23 μm diameter

rods with 300 μm diameters were used as tool electrodes. The electrodes were formed into approximately 50 μm and 23 μm diameters by the WEDG unit equipped in the experimental setup. The fabricated electrodes are shown in Fig. 17. Machining tests of high aspect ratio micro hole were then performed on RB-SiC using die-sinking EDM.

SEM micrographs of the high aspect ratio micro holes are shown in Fig. 18. An aspect ratio of 11.5 was achieved within 10 min by using 50 μm diameter tool electrode, and an aspect ratio of 21.7 micro hole was also successfully machined with the 23 μm electrode in 4 min machining time.

In order to examine the bottom surface and side wall surface integrity of high aspect ratio micro hole, the machined micro hole in Fig. 18a was dissected by a diamond cutter. Then, the sample was polished using the diamond slurry and

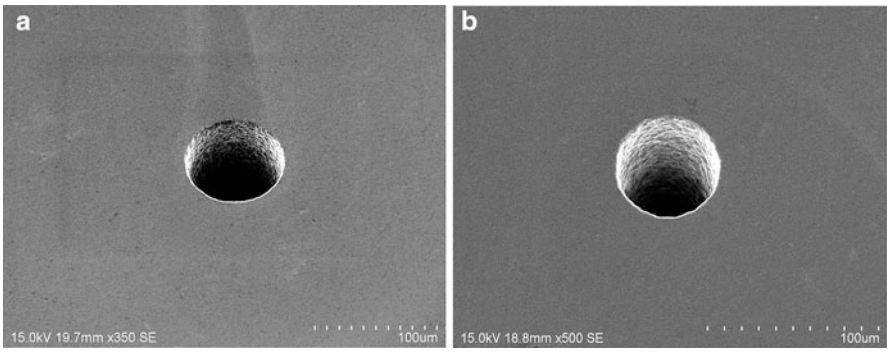

Fig. 18 High aspect ratio micro holes obtained with (**a**) 50 μm diameter tool electrode and (**b**) 23 μm diameter tool electrode

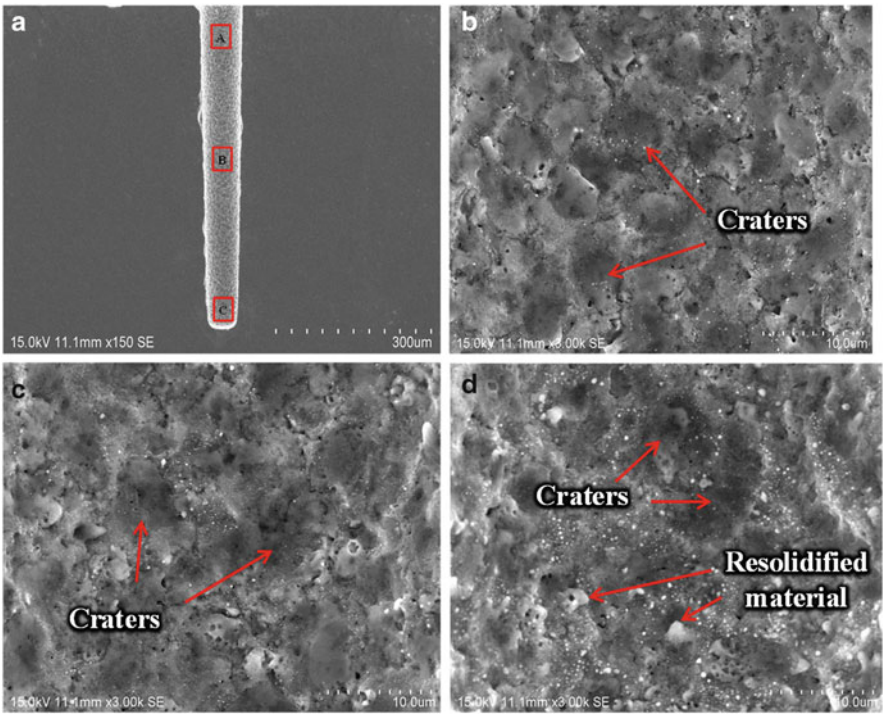

Fig. 19 SEM micrographs of (**a**) cross section of micro hole, (**b**) machined surface at zone A, (**c**) machined surface at zone B, (**d**) machined surface at zone C

subsequently observed by SEM. Figure 19a shows SEM micrograph of the cross-sectioned micro hole. It is worth noting that the bottom surface of the micro hole was flat without cone-shape protrusion even though the hole was very small and deep. Subsequently, the microstructures of the side wall of micro hole were also examined,

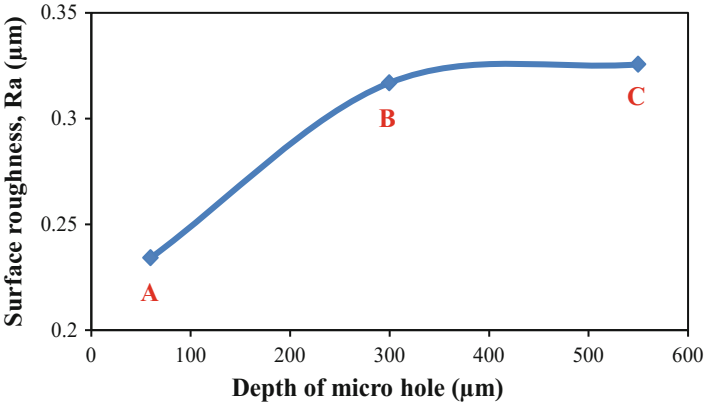

Fig. 20 Surface roughness at three locations in Fig. 19a

as shown in Fig. 19b–d. It can be seen that the side walls of micro hole were covered with overlap discharge craters and micropores which are induced by high electro-discharge energy. In addition, careful examination on the microstructures revealed that the crater sizes are increasing with the depth of the micro hole (from zone A to zone C), although this micro hole was fabricated with one parameter setting. The wall surface, especially the one in Fig. 19d, is even covered with resolidified material.

The surface roughness of hole side walls was then measured using the laser probe profilometer. The measurements were performed along the longitudinal direction at three locations as shown in Fig. 19a. Figure 20 is a plot of the change of surface roughness. It is seen that the surface roughness of the side wall increases with the depth of micro hole and the trend of which is similar to that in Fig. 19b–d. It is presumable that as the depth of micro hole increases, the debris is difficult to be flushed out, resulting in short circuit more frequently. This effect ended up with the increase of the surface roughness. On the other hand, when the hole is shallow, the debris is easily to be removed by the cavitation bubbles, leading to a better surface finish.

25.3.2.5 Fabrication of Micro Dimple Array

With the slight incline of workpiece and short fine finishing time, micro dimple array was also fabricated on RB-SiC ceramic material with the fine finishing conditions of 80 V and stray capacitance (Liew et al. 2013b). Figure 21a shows SEM micrograph of a single dimple. Figure 21b is a magnified view of the dimple surface. Clearly, the adherence of tungsten particles from electrode could be significantly suppressed by means of combination of ultrasonic cavitation and carbon nanofibers, where the amount of deposited tungsten microparticles was minimal. Good cross-sectional profile without cone-shape protrusion also can be obtained, as depicted in Fig. 21c. A measurement of surface roughness was performed across the center of the micro

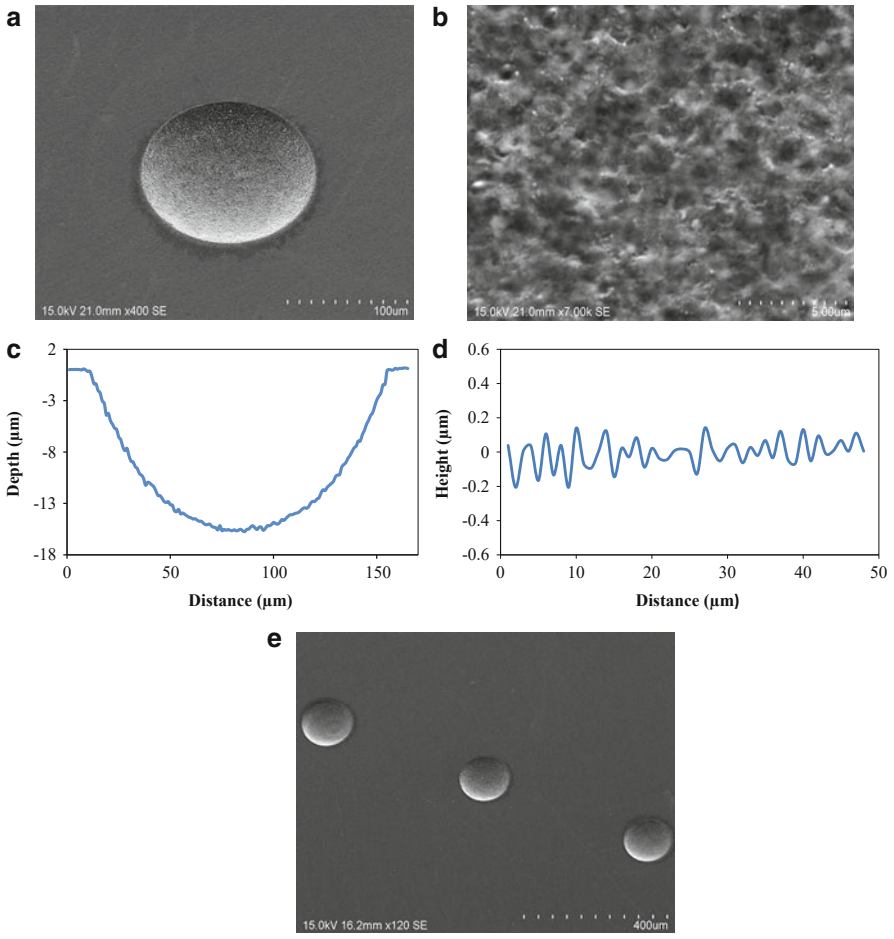

Fig. 21 Machined micro dimples obtained with hybrid process: (**a**) a single dimple, (**b**) magnified view of dimple surface, (**c**) cross-sectional profile of dimple, (**d**) surface roughness profile of dimple, and (**e**) dimple array (3 × 1)

dimple, and the evaluation length was 50 µm. The surface profile is depicted in Fig. 21d. It should be pointed out that the surface roughness of the micro dimple improved significantly, where nanometer level surface roughness (78.1 nmRa) could be obtained. Figure 21e shows SEM micrograph of a fabricated micro dimple array. These surfaces were far smoother than the one obtained without ultrasonic cavitation, as shown in Fig. 22. Without ultrasonic cavitation, tungsten electrode material was deposited on the machined surface, as depicted in Fig. 22b. The finished surface was quite rough, with a surface roughness of 0.1410 nmRa (Fig. 22c).

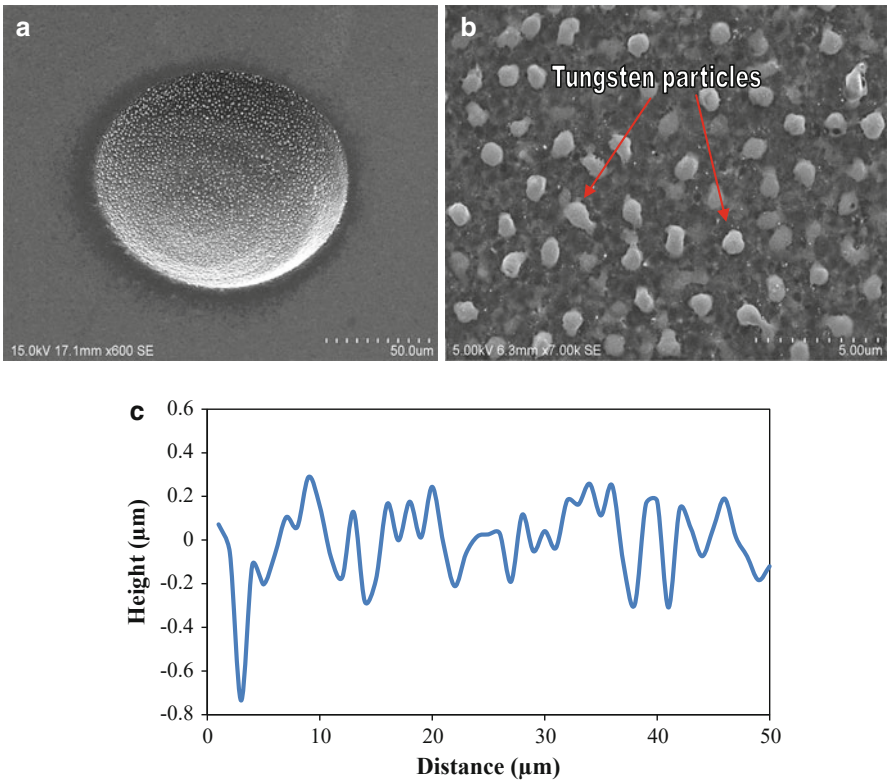

Fig. 22 Machined micro dimple without ultrasonic cavitation: (**a**) a single dimple, (**b**) magnified view of dimple surface, and (**c**) surface roughness profile of dimple

The proposed hybrid EDM process has been demonstrated to be useful for fabricating microstructures on hard brittle ceramic materials.

25.4 Hybrid Tool for EDM and Grinding

Single-crystal silicon carbide (SiC) is an excellent material for high-temperature and high-power electronic devices and microelectromechanical systems (MEMS). Compared to Si, SiC has higher thermal conductivity, current density, and breakdown electric field strength, as well as a broader band gap. However, owing to its hardness and brittleness, SiC is very difficult to machine (Tanaka and Shimada 2013). In this chapter, Yan and Tan (2015) attempted the EDM of SiC using sintered diamond (polycrystalline diamond, PCD) as a tool electrode. PCD is a composite of diamond grains sintered with a metallic binder such as Co. PCD is not only excellent for cutting and milling (Zhang et al. 2013; Katahira et al. 2014) but also useable as an electrode for EDM.

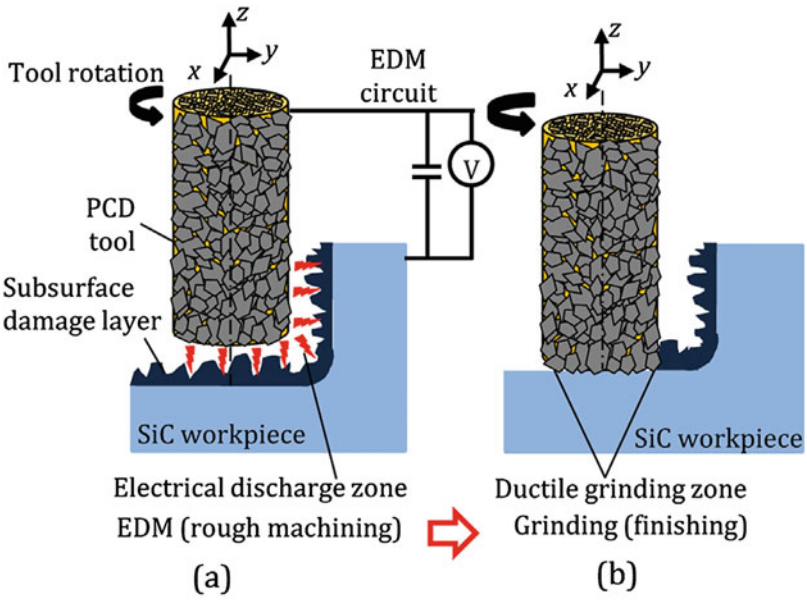

Fig. 23 Models for micromachining of SiC using a PCD hybrid tool

EDM typically creates high surface roughness and severe subsurface damage (SSD) including micro-cracks and material phase changes, as illustrated in Fig. 23a. Although the SSD layer can be removed by special polishing processes, such as plasma-assisted polishing (Yamamura et al. 2011), such polishing is very time-consuming and cannot finish three-dimensional structures or curved surfaces. Therefore, in this chapter, after EDM, the PCD electrode was used directly as a grinding wheel for finishing the EDMed surface and removing the SSD layer. Because the metallic binder in PCD is preferentially removed by electrical discharges during EDM, diamond grains protrude out of the PCD surface and act as fixed abrasive cutting edges, which remove the SSD layers efficiently through ductile mode grinding, as shown in Fig. 23b. The proposed machining process uses a single tool on a single machine and takes advantage of both the high MRR of EDM and the high surface integrity of grinding. In addition, it enables the flexible machining of three-dimensional and curved structures.

25.4.1 Experimental Methods

PCD rods with diameters of 1 mm were used as tools. It contains diamond grains with a mean size of 0.5 mm at a concentration of 90% in a Co binder, The thermal conductivity of PCD is 290 W/(m K). An n-type single-crystal 4H–SiC wafer with a surface orientation of (0 0 0 1) was used as the workpiece. The wafer was 50 mm in diameter and 0.36 mm in thickness, with a CMP finish. A micro-EDM machine (Panasonic MG-ED82 W) was used in the experiments. EDM experiments were performed at voltages of

70 and 110 V, using PCD as anode and SiC as cathode. The tool electrode's rotation rate was 3000 rpm. Both plunge grinding and mill grinding were performed using the same EDM machine and the same PCD tool. In plunge grinding, the tool feed rate in the z direction was 0.1 mm/s. In mill grinding, the depth of cut in the z direction per tool pass was 1 mm, and the tool feed rate in the y direction was set between 2.5 and 25 mm/s. The total depth of grinding was 10 mm.

25.4.2 Results of Micro-EDM

25.4.2.1 Subsurface Material Structure

Figure 24 shows cross-sectional SEM images of the EDMed surfaces. At the top of each surface, thick recast layers are clearly seen. As voltage increases from 70 to 110 V, the thickness of the recast layer increases from ~2 to ~3 mm. The results strongly demonstrate that 4H–SiC undergoes melting and resolidification during EDM, and that the local temperature in the electrical discharge zone rises above 2730 °C, the melting point of 4H–SiC.

Figure 25a shows a schematic of material removal in EDM. The high temperature generated in the electrical discharge zone (Hinduja and Kunieda 2013) causes melting and vaporization of the worked material, leaving craters on the workpiece surface. Figure 25b shows topographical changes of PCD and structural changes in SiC after EDM. Owing to the material decomposition of SiC, the workpiece undergoes surface softening. Meanwhile, the Co binder on the PCD tool surface is preferentially removed during EDM, creating chip pockets and permitting diamond grains to protrude out of the tool's surface, similar to the electrical discharge dressing of grinding wheels. These two aspects, namely, workpiece surface softening and diamond grain protrusion, are essential for the subsequent ductile mode grinding process.

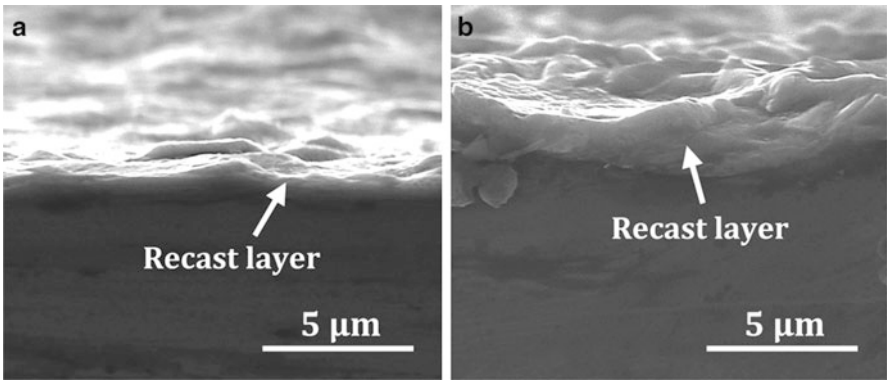

Fig. 24 Cross-sectional SEM images of EDMed surfaces at (**a**) 70 V and (**b**) 110 V, showing an increase in recast layer thickness with voltage

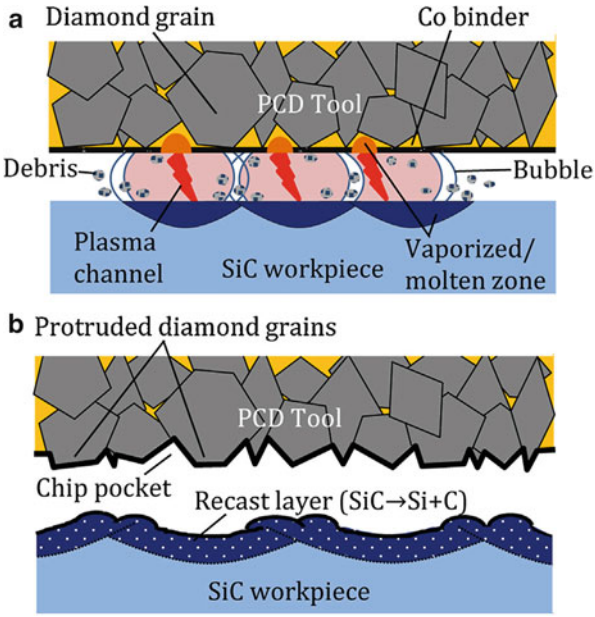

Fig. 25 Schematics of (**a**) material removal in EDM and (**b**) topographical and structural changes in both PCD and SiC

25.4.3 Results of Micro-grinding

25.4.3.1 Surface Topography Change

With the EDM power source switched off, the same PCD tool was used directly for plunge grinding tests in the SiC sample. A cut depth of 10 mm was defined in the z direction with no tool feed in the y direction. Figure 26 shows SEM images of the bottoms (a, c) and fringes (b, d) of two EDMed cavities. For the cavity EDMed at a voltage of 110 V (a, b), discharge craters were not completely removed by grinding, indicating that the SSD was deeper than 10 mm. For the cavity EDMed at 70 V (c, d), however, craters are barely visible, with only grinding marks evident on the surface.

25.4.3.2 Effects of Transverse Tool Feed

To eliminate the grinding marks formed via plunge grinding, as shown in Fig. 26, mill grinding was performed by traverse feeding the PCD tool in the y direction. Figure 27a is a micrograph of an EDMed micro-cavity. The surface is rough with dense discharge craters. Figure 27b shows an EDMed and then mill-ground micro-cavity at a traverse tool feed rate of 25 mm/s. The surface appears as smooth as the surrounding area finished by CMP. The time for EDM was 8.1 min and that for grinding was 7.3 min, respectively.

25.4.3.3 Comparison of Surface Roughness

Figure 28 shows a plot of surface roughness after different process steps. The surface roughness of an as-received 4H–SiC wafer with a CMP finish is also shown for

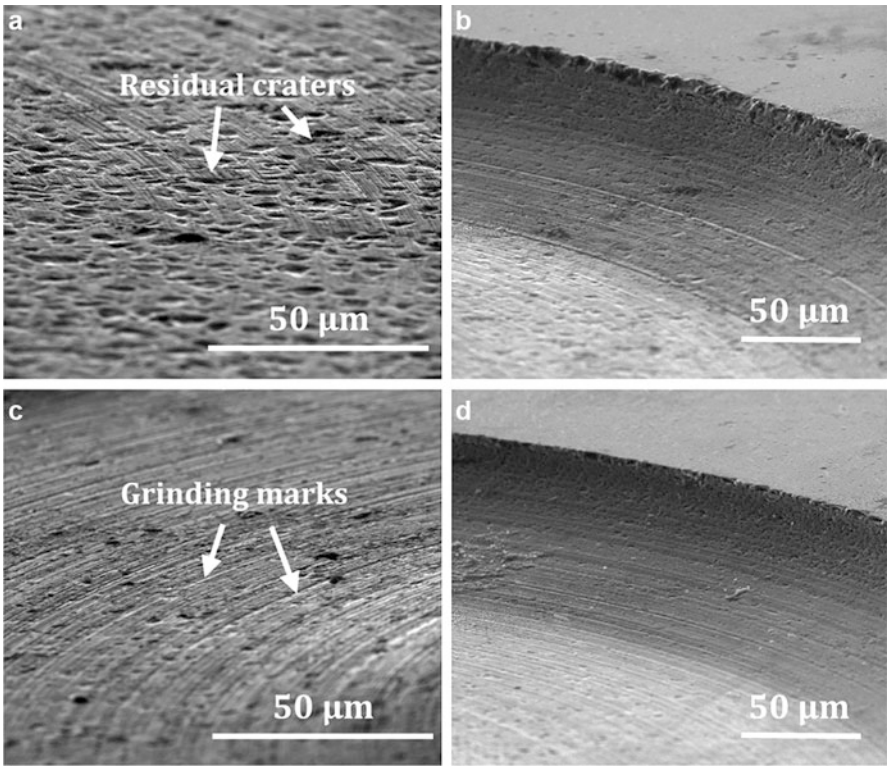

Fig. 26 SEM images of the bottoms (**a**, **c**) and fringes (**b**, **d**) of EDMed cavities after plunge grinding. The voltages used in EDM were (**a**, **b**) 110 V and (**c**, **d**) 70 V

comparison. The surface roughness Ra after EDM was 417 nm (Sa = 439 nm). After mill grinding, however, Ra decreased to 1.85 nm (Sa = 2.60 nm), a factor of 200 less than that of the EDMed surface. The surface quality resulting from the proposed process approaches is achieved by CMP, while the processing time is distinctly shorter than that of CMP.

25.5 Summary and Outlook

In this chapter, a comprehensive review on the micro-EDM of hard and brittle ceramic materials was presented. Three main methods that are commonly used to improve the machining efficiency of hard and brittle ceramic materials were powder mixed EDM, assisting electrode EDM and electrical discharge milling and mechanical grinding. Following the review, a few recently developed technologies in this area were introduced. For example, adding carbon nanofibers into the dielectric fluid can significantly improve the spark gap and material removal rate compared to that

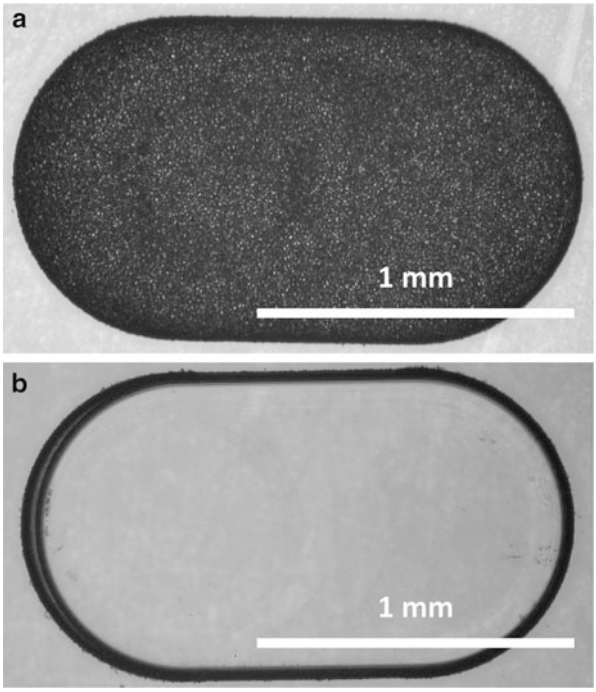

Fig. 27 Micrographs of (**a**) an EDMed cavity and (**b**) an EDMed and then mill-ground cavity by introducing a traverse tool feed

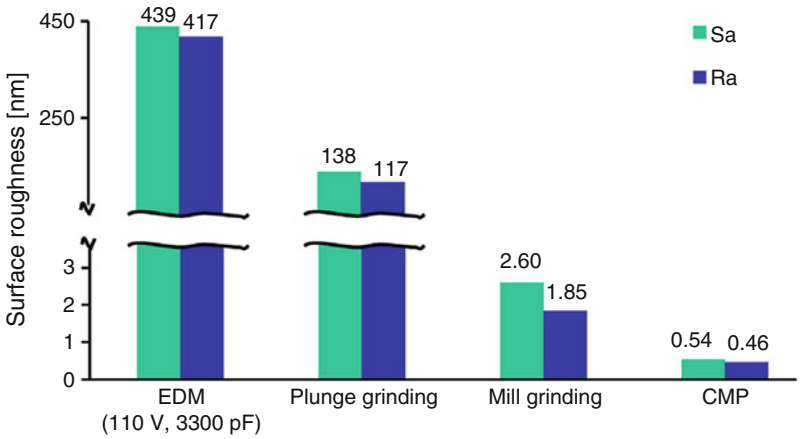

Fig. 28 Comparison of surface roughness resulting from different process steps using the PCD hybrid tool versus CMP

of spherical carbon powder. Ultrasonic cavitation assisted micro-EDM with carbon nanofibers addition in the dielectric fluid can distinctly improve the form accuracy, depth, and surface finish of the micro hole. The hybrid micro-EDM process can be applied to machine high aspect ratio micro holes and micro dimple array on hard

brittle RB-SiC ceramic material. Finally, a novel hybrid tooling technology was introduced by using sintered diamond (polycrystalline diamond, PCD) as a hybrid tool for EDM and grinding. An extremely smooth surface (Ra = 1.85 nm) was obtained on single-crystal SiC after EDM using the same tool.

Micro-EDM is a promising technology that can cater to the growing demands for miniaturization in various industrial sectors. Compared to other traditional machining technologies, micro-EDM requires a low installation cost, and it can machine complex or 3D micro shapes easily. Furthermore, micro-EDM is very flexible and suitable for prototypes with high added value. Future developments in the area of micro-EDM of hard and brittle materials would be focused on the development of control algorithms and power supply, analysis of energy consumption, surface alloying/coating on complicated shapes, predictive modeling of the process, and so on. Intensive studies on these aspects would help to overcome the difficulties associated with shaping the single crystals and ceramics parts.

References

Brennen CE (1995) Cavitation and bubble dynamics. Oxford University Press, New York

Chow HM, Yang LD, Lin CT et al (2008) The use of SiC powder in water as dielectric for micro-slit EDM machining. J Mater Process Technol 195:160–170

Chung DK, Shin HS, Park MS et al (2011) Recent researches in micro electrical machining. Int J Precis Eng Manuf 12(2):371–380

Clijsters S, Liu K, Reynaerts D et al (2010) EDM technology and strategy development for the manufacturing of complex parts in SiSiC. J Mater Process Technol 210:631–641

Descoeudres A (2006) Characterization of electrical discharge machining plasmas. Ecole Polytechnique Federale De Lausanne PhD's Thesis

Ekmekci B, Sayar A (2013) Debris and consequences in micro electric discharge machining of micro-holes. Int J Mach Tool Manu 65:58–67

Fukuzawa Y, Mohri N, Tani T et al (2004) Electrical discharge machining properties of noble crystals. J Mater Process Technol 149:393–397

Fukuzawa Y, Mohri N, Gotoh H et al (2009) Three-dimensional machining of insulating ceramics materials with electrical discharge machining. Trans Nonferrous Met Soc China 19:s150–s156

Gotoh H, Tani T, Mohri N (2016) EDM of insulating ceramics by electrical conductive surface layer control. Procedia CIRP 42:201–205

Gunawan SP, Mahardika M, Hamdi M et al (2009) Effect of micro-powder suspension and ultrasonic vibration of dielectric fluid in micro-EDM processes-Taguchi approach. Int J Mach Tool Manu 49:1035–1041

Gunawan SP, Muslim M, Hamdi M et al (2011) Accuracy improvement in nanographite powder-suspension dielectric fluid for micro-electrical discharge machining process. Int J Adv Manuf Technol 56:143–149

Hinduja S, Kunieda M (2013) Modelling of ECM and EDM processes. CIRP Ann 62(2):775–797

Ho KH, Newman ST (2003) State of the art electrical discharge machining (EDM). Int J Mach Tool Manu 43:1287–1300

Hung JC, Lin JK, Yan BH et al (2006) Using a helical micro-tool in micro-EDM combined with ultrasonic vibration for micro-hole machining. J Micromech Microeng 16:2705–2713

Jahan M, Rahman M, Wong YS (2010a) Modelling and experimental investigation on the effect of nanopowder-mixed dielectric in micro-electrodischarge machining of tungsten carbide. Proc Inst Mech Eng B 224(11):1725–1739

Jahan M, Rahman M, Wong YS (2010b) Study on the nano-powder-mixed sinking and milling micro-EDM of WC-Co. Int J Adv Manuf Technol 53:167–180
Ji R, Liu Y, Zhang Y et al (2010) Machining performance and surface integrity of SiC ceramic machined using electrical discharge milling and the mechanical grinding compound process. Proc Inst Mech Eng B 224:1511–1518
Ji R, Liu Y, Zhang Y et al (2011) Machining performance of silicon carbide ceramic in end electric discharge milling. Int J Refract Met Hard Mater 29:117–122
Kalpakjian S, Schmid SR (2001) Manufacturing engineering and technology, 4th edn. Prentice-Hall, Upper Saddle River, Pearson Publisher, New Jersey
Kansal HK, Singh S, Kumar P (2007) Effect of silicon powder mixed EDM on machining rate of AISI D2 die steel. J Manuf Process 9(1):13–22
Katahira K, Takesue S, Komotori J et al (2014) Micromilling characteristics and electrochemically assisted reconditioning of polycrystalline diamond tool surfaces for ultra-precision machining of high-purity SiC. CIRP Ann 63(1):329–332
Konig W, Dauw DF, Levy G et al (1988) EDM-future steps towards the machining of ceramics. CIRP Ann 37(2):623–631
Kumar S, Brennen CE (1991) Nonlinear effects in the dynamics of clouds of bubbles. J Acoust Soc Am 89:707–714
Lee S, Scarpulla MA, Bamberg E (2013) Effect of metal coating on machining of high purity germanium using wire electrical discharge machining. J Mater Process Technol 213:811–817
Liew PJ, Yan J, Kuriyagawa T (2013a) Carbon nanofiber assisted micro electro discharge machining of reaction-bonded silicon carbide. J Mater Process Technol 213(7):1076–1087
Liew PJ, Shimada K, Mizutani M et al (2013b) Fabrication of microstructures on RB-SiC by ultrasonic cavitation assisted micro-electrical discharge machining. Int J Automot Technol 7(6):621–629
Liew PJ, Yan J, Kuriyagawa T (2014) Fabrication of deep micro-holes in reaction-bonded SiC by ultrasonic cavitation assisted micro-EDM. Int J Mach Tool Manu 76:13–20
Liu Y, Ji R, Li Q et al (2008) Electrical discharge milling of silicon carbide ceramic with high electrical resistivity. Int J Mach Tools Manuf 48:1504–1508
Liu Y, Ji R, Li Q et al (2009) An experimental investigation for electric discharge milling of SiC ceramics with high electrical resistivity. J Alloys Compd 472:406–410
Masuzawa T (2000) State of the art of micromachining. CIRP Ann 49:473–488
Masuzawa T, Fujino M, Kobayashi K et al (1985) Wire electro-discharge grinding for micro-machining. CIRP Ann 34(1):431–434
Mohri N, Fukuzawa Y, Tani T et al (1996) Assisting electrode method for machining insulating ceramics. CIRP Ann 45(1):201–204
Morgan CJ (2004) Micro electro-discharge machining: techniques and procedures for micro fabrication. Master's thesis, University of Kentucky
Muttamara A, Fukuzawa Y, Mohri N et al (2003) Probability of precision micro-machining of insulating Si_3N_4 ceramics by EDM. J Mater Process Technol 140:243–247
Muttamara A, Fukuzawa Y, Mohri N et al (2009) Effect of electrode material on electrical discharge machining of alumina. J Mater Process Technol 209:2545–2552
Pham DT, Dimov SS, Bigot S et al (2004) Micro-EDM-recent developments and research issues. J Mater Process Technol 149:50–57
Puertas I, Luis CJ (2004) A study on the electrical discharge machining of conductive ceramics. J Mater Process Technol 153-154:1033–1038
Reynaerts D, Meeusen W, Brussel HV (1998) Machining of three-dimensional microstructures in silicon by electro-discharge machining. Sensor Actuator A 67:159–165
Sabur A, Ali MY, Maleque MA et al (2013) Investigation of material removal characteristics in EDM of nonconductive ZrO_2 ceramic. Procedia Eng 56:696–701
Schumacher BM (2004) After 60 years of EDM the discharge process remains still disputed. J Mater Process Technol 149:376–381
Suslick KS (1989) The chemical effects of ultrasound. Sci Am 260:80–86
Tanaka H, Shimada S (2013) Damage-free machining of monocrystalline silicon carbide. CIRP Ann 62(1):55–58

Tani T, Fukuzawa Y, Nanbu K, Mohri N (2002) Machining phenomena in EDM of insulating ceramics with powder mixed oil. J Jpn Soc Elec Mach Eng 36(81):39–46
Tani T, Fukuzawa Y, Mohri N, Saito N, Okada M (2004) Machining phenomena in WEDM of insulating ceramics. J Mater Process Technol 149(1–3):124–128
Wang J, Han F, Cheng G, Zhao F (2012) Debris and bubble movements during electrical discharge machining. Int J Mach Tools Manuf 58:11–18
Yamamura K, Takiguchi T, Ueda M et al (2011) Plasma assisted polishing of single crystal SiC for obtaining atomically flat strain- free surface. CIRP Ann 60(1):571–574
Yan J, Tan TH (2015) Sintered diamond as a hybrid EDM and grinding tool for the micromachining of single-crystal SiC. CIRP Ann Manuf Technol 64:221–224
Yeo SH, Tan PC, Kurnia W (2007) Effects of powder additives suspended in dielectric on crater characteristics for micro electrical discharge machining. J Micromech Microeng 17:N91–N98
Yi SM, Park MS, Lee YS et al (2008) Fabrication of a stainless steel shadow mask using batch mode micro-EDM. Microsyst Technol 14(3):411–417
Yu ZY, Zhang Y, Li J et al (2009) High aspect ratio micro-hole drilling aided with ultrasonic vibration and planetary movement of electrode by micro-EDM. CIRP Ann Manuf Technol 58:213–216
Zahiruddin M, Kunieda M (2012) Comparison of energy and removal efficiencies between micro and macro EDM. CIRP Ann – Manuf Technol 61:187–190
Zhang Z, Peng H, Yan J (2013) Micro-cutting characteristics of EDM fabricated high-precision polycrystalline diamond tools. Int J Mach Tools Manuf 65:99–106